

# Physical map of chromosomal nitrogen fixation (*nif*) genes of *Klebsiella pneumoniae*

(transposable elements/restriction mapping/recombinant DNA)

GERARD E. RIEDEL\*, FREDERICK M. AUSUBEL\*, AND FRANK C. CANNON†

\*Department of Biology, Harvard University, Cambridge, Massachusetts 02138; and †Agricultural Research Council Unit of Nitrogen Fixation, University of Sussex, Falmer, Brighton BN1 9QJ, United Kingdom

Communicated by A. M. Pappenheimer, Jr., March 1, 1979

**ABSTRACT** We describe a method for the rapid determination of the physical location of mutations caused by insertion of transposable elements. We used this method to construct a detailed physical map of the nitrogen fixation (*nif*) gene cluster of *Klebsiella pneumoniae* and to correlate it with the genetic map. Total cellular DNA was isolated from individual strains, each carrying an insertion in 1 of 15 different *nif* genes. The DNA was digested with a restriction endonuclease, fractionated by agarose gel electrophoresis, denatured, and blotted onto nitrocellulose filter paper. The DNA on the filters was hybridized with <sup>32</sup>P-labeled DNA fragments derived from amplifiable plasmids carrying cloned *nif* DNA fragments from *K. pneumoniae*. Altered hybridization patterns caused by insertions into *nif* genes allowed us to map *nif* mutations with respect to the previously mapped cleavage sites for various restriction endonucleases. We have used the same method to map the end points of *nif* deletions. Using this procedure, we assigned physical locations on the *K. pneumoniae* chromosome to 86 *nif* insertion mutations and 13 *nif* deletion end points. This mapping procedure provides a convenient alternative to deletion mapping as a definitive method for mapping insertion mutations within a gene or for ordering genes within a gene cluster. This procedure will be especially useful for mapping mutations conferring phenotypes that are difficult to monitor and for mapping mutations in bacterial species in which techniques for conducting deletion mapping have not been devised.

Genes specifically required for the fixation of dinitrogen (N<sub>2</sub>) in *Klebsiella pneumoniae* are clustered on the genetic map near the operator end of the histidine biosynthesis (*his*) operon (1-7). Fifteen distinct nitrogen fixation (*nif*) genes have been identified in this cluster on the basis of complementation analysis (refs. 1-3; R. Dixon, M. Filser, and M. Merrick, personal communication). We have previously described the construction, *in vitro*, of amplifiable plasmids that carry the *hisGD* genes and 14 of the 15 known *nif* genes (8, 9).

Using the amplifiable *nif* plasmids in complementation and marker rescue tests, we have been able to construct a map that roughly locates the *nif* genes with respect to the cleavage sites of several restriction endonucleases (8, 9). These techniques, however, revealed a little about the specific location of each *nif* gene on the chromosome. Therefore, we have devised an alternative method for determining the location of mutations (insertions and deletion end points) on a DNA restriction fragment of the chromosome. In addition to ordering the insertion mutations unambiguously, the method allows an estimation of the minimal size of individual genes and identifies restriction fragments that carry specific genes or portions of specific genes. This mapping procedure is a logical extension of the use of transposable elements for mapping plasmids (10-12).

The publication costs of this article were defrayed in part by page charge payment. This article must therefore be hereby marked "advertisement" in accordance with 18 U. S. C. §1734 solely to indicate this fact.

## MATERIALS AND METHODS

**Bacterial Strains.** *Escherichia coli* K-12 strain FMA185 is W3110 (13) *recA hsp hisD gal*; *E. coli* strain JC5466 (14) is *his trp recA spec. Klebsiella pneumoniae nif* deletion strains UNF 126, 128, 131, 134, 155, 156, 168, and 169 and *nif* inversion strain 2042 were supplied by R. Dixon and some are described in ref. 2. *K. pneumoniae nif* deletion strain KP52 was from S. Streicher (15). *K. pneumoniae* strain KP5022 is *hisD hsp* (8), and *K. pneumoniae* strain UN2454 (*nifQ5027::Muc<sup>ts</sup>61*) was obtained from W. Brill (1). *K. pneumoniae* strains UNF 143, 2038, 2040, and 2027, containing Tn10 insertions in *nif* genes, were obtained from R. Dixon (2).

**Conjugative Plasmids.** pRD1 (16) carries the *his-nif* region of the *K. pneumoniae* chromosome and confers tetracycline, ampicillin, and kanamycin resistance. pMF1 (2) carries the complete *his* and *nif* gene clusters from pRD1 but does not confer any drug resistances. Tn5 and Tn10 insertions into pMF1 were provided by M. Filser and by R. Dixon and M. Merrick, respectively. Some of these pMF1 derivatives are described in ref. 2. Bacteriophage Mu insertions into pCE1, a pRD1 derivative that no longer confers Mu resistance to its host, and Mu-induced deletions in pCE1 were provided by C. Elmerich. Some of these are described in ref. 3.

**Amplifiable Plasmids.** Restriction fragments of the *his* and *nif* regions of the *K. pneumoniae* chromosome that have been cloned in plasmids and used in this work are shown in Fig. 1. Plasmids pCRA37, pCM1, and pSA30 have been described (8, 9). Plasmids pGR102, 103, and 104 are deletion derivatives of pCRA37 generated *in vitro* by using restriction enzyme techniques. Plasmids pGR112 and 113 contain *EcoRI* fragments that were originally cloned in pCRA37 and pCM1, respectively.

The plasmids were constructed and purified in a P2 containment laboratory, in accordance with the National Institutes of Health Guidelines for Recombinant DNA Research. Details of plasmid constructions will be reported elsewhere.

**Transposable Elements.** Restriction maps for bacteriophage Mu (17), and for transposons Tn5 (ref. 18; R. Jorgensen and W. Reznikoff, personal communication) and Tn10 (19) are shown in Fig. 1.

**DNA Isolation.** Strain JC5466 carrying Nif<sup>-</sup> derivatives of pRD1 or pMF1 and *K. pneumoniae nif*<sup>+</sup> and *nif* deletion strains were grown to saturation in basal salts medium (8) supplemented with each required amino acid at 50 μg/ml. Total DNA was isolated from 5 ml of culture by using a simplified version of the method described by Marmur (20). Supercoiled plasmid DNAs were isolated from strain FMA185 and purified as described (8).

Abbreviation: kb, kilobase(s).

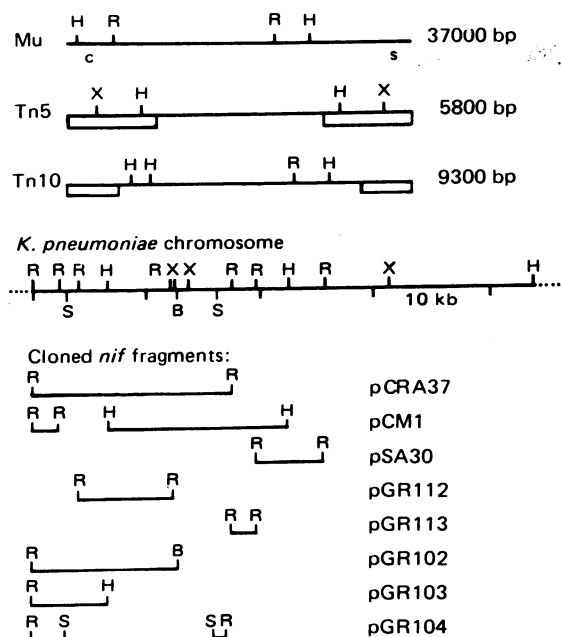


FIG. 1. Transposable elements and amplifiable plasmids used in this study. On the restriction map of bacteriophage Mu (17), the letters "c" and "s" below the map orient the map with respect to the genetic map (17). For restriction maps of Tn5 (ref. 18; R. Jorgensen and W. Reznikoff, personal communication) and Tn10 (19), the boxed regions at the ends denote the inverted repeat regions of 1460 and 1400 base pairs (bp), respectively. The details of the construction of the restriction map of the *his-nif* region of the *K. pneumoniae* chromosome will be reported elsewhere. The different *nif* fragments have been cloned in amplifiable plasmids. R, *EcoRI*; H, *HindIII*; X, *Xho I*; B, *BamHI*; S, *Sal I*.

**DNA Biochemistry.** For restriction digestion of total cellular DNA, 2  $\mu$ g of DNA was incubated with 10 units of enzyme for 3–5 hr. Restriction endonuclease *EcoRI* was purified and used as described (21). *Sal I* was a gift from J. Bedbrook; *BamHI*, *HindIII*, *Xho I*, and *Bgl II* were purchased from Bethesda Research Laboratories (Rockville, MD) and used according to the manufacturer's specifications. Digested DNA was fractionated by electrophoresis in a horizontal 1% agarose gel (20  $\times$  14  $\times$  0.8 cm) with 12 slots (9  $\times$  7.5  $\times$  1.5 mm); electrophoresis was in SEB buffer (8) for 12–16 hr at a constant current of 30–50 mA. The gels were stained and photographed as described (8). DNA was transferred from the agarose slab gels to nitrocellulose filter paper (Schleicher & Schuell, type BA85) by the method of Southern (22).  $^{32}$ P-Labeled hybridization probes were prepared from purified plasmid DNA [or a purified restriction fragment (23)] by "nick translation" (24, 25) using thymidine 5'-[ $\alpha$ - $^{32}$ P]triphosphate (350 Ci/mmol; 1 Ci =  $3.7 \times 10^{10}$  becquerels) from Amersham and DNA polymerase I from Boehringer Mannheim. Hybridization of the probes to the nitrocellulose filters and the subsequent washing of the filters were performed as described (26–28). A typical hybridization experiment used 0.2  $\mu$ g of  $^{32}$ P-labeled DNA at a specific activity of  $5 \times 10^7$  dpm/ $\mu$ g of DNA for a nitrocellulose filter containing 12 DNA digests. Kodak XR-1 film was exposed for 4–48 hr.

**Experimental Plan.** The goal of the experiments described in this paper was to determine the location of each *nif* gene with respect to mapped sites for restriction endonucleases in the *nif* gene cluster. Our overall plan was to monitor alterations of *nif* DNA restriction fragments in strains containing various *nif* deletions (2, 3) or in strains carrying Tn5, Tn10, or phage Mu insertions in various *nif* genes (1–3). The extent of each deletion had been determined by marker rescue tests (2, 3) and each insertion had been assigned a location within 1 of the 15 genes in the *nif* cluster on the basis of complementation or deletion

mapping analysis or both (refs. 1 and 3; R. Dixon, M. Filser, and M. Merrick, personal communication).

Our strategy used the following steps: (i) isolation of total cellular DNA from *nif* mutant strains; (ii) digestion of the DNA with a restriction endonuclease; (iii) fractionation of the fragments by agarose gel electrophoresis; (iv) transfer of the DNA fragments to nitrocellulose filter paper; and (v) analysis by hybridization with a  $^{32}$ P-labeled DNA fragment derived from a plasmid carrying *nif* genes. Altered hybridization patterns caused by the insertions or deletions permitted construction of a physical map of the location of *nif* insertions and *nif* deletion end points. In each case we first identified specific restriction fragments containing the insertion or deletion end point and then, in a second step, determined more precisely the point of insertion or deletion within that fragment.

In both steps, we used: (i) plasmids that we constructed carrying various regions of the *nif* cluster, (ii) a restriction map of the *nif* gene cluster derived from restriction endonuclease analysis of amplifiable *nif* plasmid DNA, and (iii) restriction maps of Tn5, Tn10, and phage Mu. These plasmids and restriction maps are depicted in Fig. 1. (See also Fig. 5 for correlation with the genetic map.)

## RESULTS

**Mapping Insertions in Chromosomal DNA Sequences Homologous to Cloned DNA Sequences.** The transposon Tn5 [5.8 kilobases (kb)] contains no recognition site for *EcoRI*. Therefore, an *EcoRI* digest of total cellular DNA from a strain carrying Tn5 inserted in *nifB*, for example (see Fig. 2), should contain one *nif EcoRI* fragment that is larger by 5.8 kb. In Fig. 2, the "altered restriction fragment" was detected by hybridization of a "Southern filter blot" (22) of the *EcoRI*-digested DNA with  $^{32}$ P-labeled pCRA37 DNA, a plasmid that carries four contiguous *EcoRI* fragments of the *his-nif* region of *K. pneumoniae* (See Fig. 1). Comparison of the hybridization patterns in lanes C and D of Fig. 2 shows that Tn5 is inserted into the largest (labeled "I") of the four *EcoRI* fragments contained in pCRA37.

In order to determine the location of the *nifB*:Tn5 insertion within *EcoRI* fragment I more precisely, total cellular DNA containing the Tn5 insertion was cleaved with both *EcoRI* and *Xho I*. *Xho I* does not cleave *EcoRI* fragment I but does cleave Tn5 within the terminally repeated DNA sequences (see Fig. 1), leaving two identical 0.5-kb Tn5 segments attached to the "left" and "right" portions of *nif EcoRI* fragment I. As shown in Fig. 2 lanes E and F, filter hybridization of the doubly digested DNA with  $^{32}$ P-labeled pGR112, a plasmid containing only *EcoRI* fragment I, revealed the disappearance of the wild-type *EcoRI* fragment I and the appearance of two new fragments. The combined size of these two new fragments (4.6 and 4.3 kb) equals the size of wild-type *EcoRI* fragment I (7.95 kb) plus the two 0.5-kb pieces of Tn5 attached to the *nif* sequences. By subtracting 0.5 kb from the size of these two new fragments, we calculated that Tn5 was inserted 3.8 kb from one end of fragment I and 4.1 kb from the other end. The data thus far did not distinguish which fragments (4.6 or 4.3 kb) corresponded to the "left" and the "right" portions of *nif EcoRI* fragment I. The "left" and "right" fragments were readily distinguished by analyzing a duplicate nitrocellulose filter of the doubly digested DNA with  $^{32}$ P-labeled pGR103, a plasmid bearing homology only to the "left" half of *EcoRI* fragment I. Fig. 2 lane H shows that the smaller DNA fragment is the "left" end of *EcoRI* fragment I. Thus, the Tn5 insertion in *nifB* is located 3.8 kb from the left end of *EcoRI* fragment I.

The method illustrated in Fig. 2 for mapping a Tn5 insertion in *nifB* is an example of one of the specific strategies we used to map Tn5, Tn10, and Mu insertions. The procedure used in

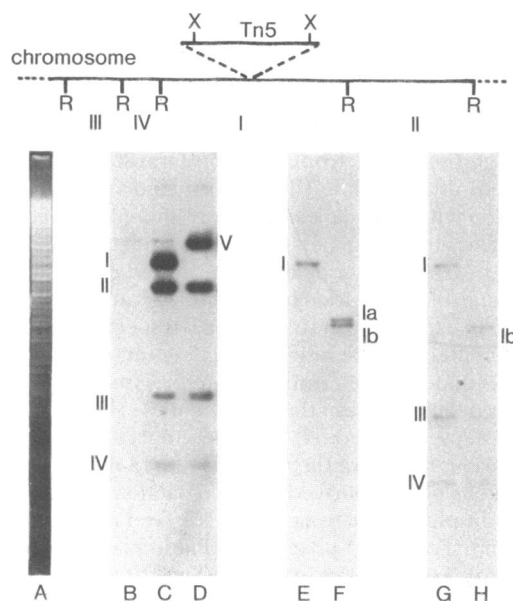


FIG. 2. Hybridization of  $^{32}\text{P}$ -labeled *nif* fragments to DNA from a bacterial strain containing a Tn5 insertion in the *nifB* gene. (Upper) Diagram of the *EcoRI* recognition sites in the region of the *K. pneumoniae* chromosome near the site of the insertion of Tn5 into *nifB*. R, *EcoRI*; X, *Xho* I. (Lower) Lanes: A, agarose gel electrophoresis of an *EcoRI*-digest of 2  $\mu\text{g}$  of total DNA isolated from JC5466/pMF1::Tn5. Electrophoresis was for 16 hr in 1% agarose at constant current (35 mA). B-H, Autoradiograms of  $^{32}\text{P}$  *nif* DNA fragments hybridized to restriction digests of total DNA isolated from JC5466 (lane B), JC5466/pMF1::Tn5 (lanes C, E, and G), and JC5466/pMF1 *nifB*::Tn5 (lanes D, F, and H). The DNA in lanes A, B, C, and D was digested with *EcoRI*; that in lanes E, F, G, and H was doubly digested with *EcoRI* and *Xho* I. The hybridization probes used in these experiments were: lanes B, C, and D, [ $^{32}\text{P}$ ]pCRA37 which is homologous to fragments I, II, III, and IV above; lanes E and F, [ $^{32}\text{P}$ ]pGR112 which is homologous only to fragment I; and lanes G and H, [ $^{32}\text{P}$ ]pGR103 which is homologous to fragments III and IV and the "left" portion of fragment I. Additional explanations of this experiment are provided in the text. The faint hybridization band present at the top of lanes B and C represents a DNA fragment from the JC5466 DNA which is homologous to the pCRA37 hybridization probe.

other cases depended upon the transposable element and the restriction enzyme recognition sites that we had mapped in the vicinity of each insertion. Because Tn10 and Mu are both cleaved asymmetrically by *EcoRI* and because this asymmetry is large (see Fig. 1), we were able to determine the orientation as well as the location of each Tn10 and Mu insertion.

**Mapping Insertions in Chromosomal DNA Sequences Adjacent to Cloned DNA Sequences.** We have examined DNA from 15 strains carrying Tn5, Tn10, and bacteriophage Mu insertions that were determined to be *nifJ* by complementation analysis (refs. 2 and 3; R. Dixon, M. Filser, and M. Merrick, personal communication). In all 15 cases, we found that the insertions were outside of the *nif* region defined by the segments cloned in our collection of plasmids (depicted in Fig. 1). Genetic mapping data place *nifJ* to the right of *nifH* (see Fig. 4). Therefore, it was likely that insertions in *nifJ* mapped to the right of the *EcoRI* fragment cloned in pSA30 but mapped within a large (21 kb) *HindIII* fragment shown at the top of Fig. 3. Because part of the 21-kb *HindIII* fragment is present in pSA30, this plasmid could be used as a hybridization probe to monitor alterations of the 21-kb *HindIII* fragment caused by the 15 insertions in *nifJ*. Autoradiography revealed that the 21-kb *HindIII* fragment present in wild-type DNA (fragment I, Fig. 3) was absent from the DNA of all the strains containing insertions in *nifJ* and that new fragments appeared in each of the DNA digests (see Fig. 3, lanes B-K). As diagrammed in the

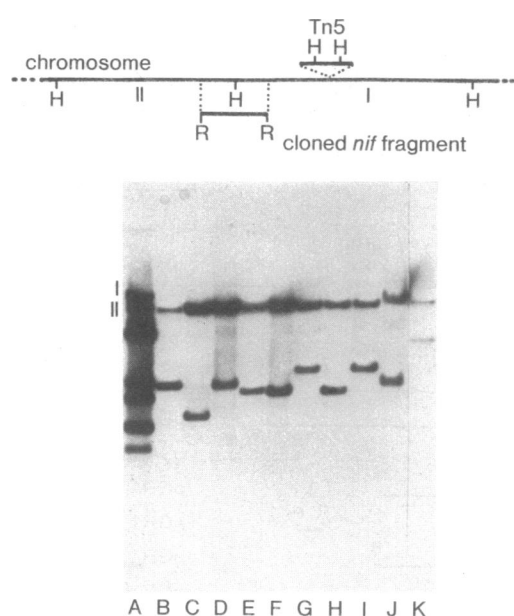


FIG. 3. Autoradiogram of  $^{32}\text{P}$ -labeled pSA30 hybridized to *HindIII* digests of total DNA isolated from bacterial strains containing insertions in *nifJ*. (Upper) Restriction map of the *nifJ* region in the vicinity of insertions of transposable elements into *nifJ*. An example of a Tn5 insertion is depicted. The region corresponding to the *EcoRI* fragment cloned in pSA30 is depicted to illustrate homology with the chromosomal *HindIII* fragments I and II. H, *HindIII*; R, *EcoRI*. (Lower) Autoradiogram of [ $^{32}\text{P}$ ]pSA30 DNA hybridized to *HindIII* digests of total DNA isolated from various sources: A, JC5466/pMF1::Tn5; B-I, JC5466 containing independently isolated pMF1 derivatives with a Tn5 insertion in *nifJ*; J, JC5466/pRD1*nifJ*::Muc<sup>+</sup>; K, *K. pneumoniae* strain 2027 (*nifJ*::Tn10). The additional hybridization bands in lane A correspond to DNA fragments added to the *HindIII* digest of JC5466/pMF1::Tn5 DNA. These fragments share homology with the pSA30 hybridization probe and serve as molecular weight markers.

top of Fig. 3, the insertion of Tn5 introduces new *HindIII* restriction recognition sites into the mutant strains, allowing us to calculate the distance between the site of insertion of the transposable elements and the *HindIII* recognition site within the *EcoRI* fragment cloned in pSA30. In the case of Tn10 and Mu, which also introduce new *HindIII* recognition sites, we determined the orientation of the transposable element by hybridizing a duplicate *HindIII* digest with a probe that was homologous to the "left" or "right" portion of Tn10 or Mu (data not shown).

**Mapping the End-Point Regions of Deletions.** Because deletions are the loss of DNA from the chromosome, the restriction map of the region around the end point of a deletion should be different from the restriction map of the corresponding wild-type region. We made use of this feature of deletions to determine the end-point region for several *nif* deletions.

Total DNA was isolated from *nif* deletion strains, cleaved with *EcoRI*, and analyzed, as described above, by using a mixture of  $^{32}\text{P}$ -labeled pCRA37, pGR113, and pSA30 DNA. These probes contain the total length of the *his-nif* region in our clone collection. The hybridization pattern of the *nif* deletion DNA was compared to the hybridization pattern of the *nif* wild-type DNA. In all cases, the DNA from *nif* deletion strains lacked one or more of the fragments that were present in the wild-type DNA; analysis of the fragments that were missing enabled us to determine the *EcoRI* fragment in which the deletion ended and the direction in which the deletion extended. We also cleaved *nif* deletion strains with several other restriction enzymes which allowed us to assign a region between

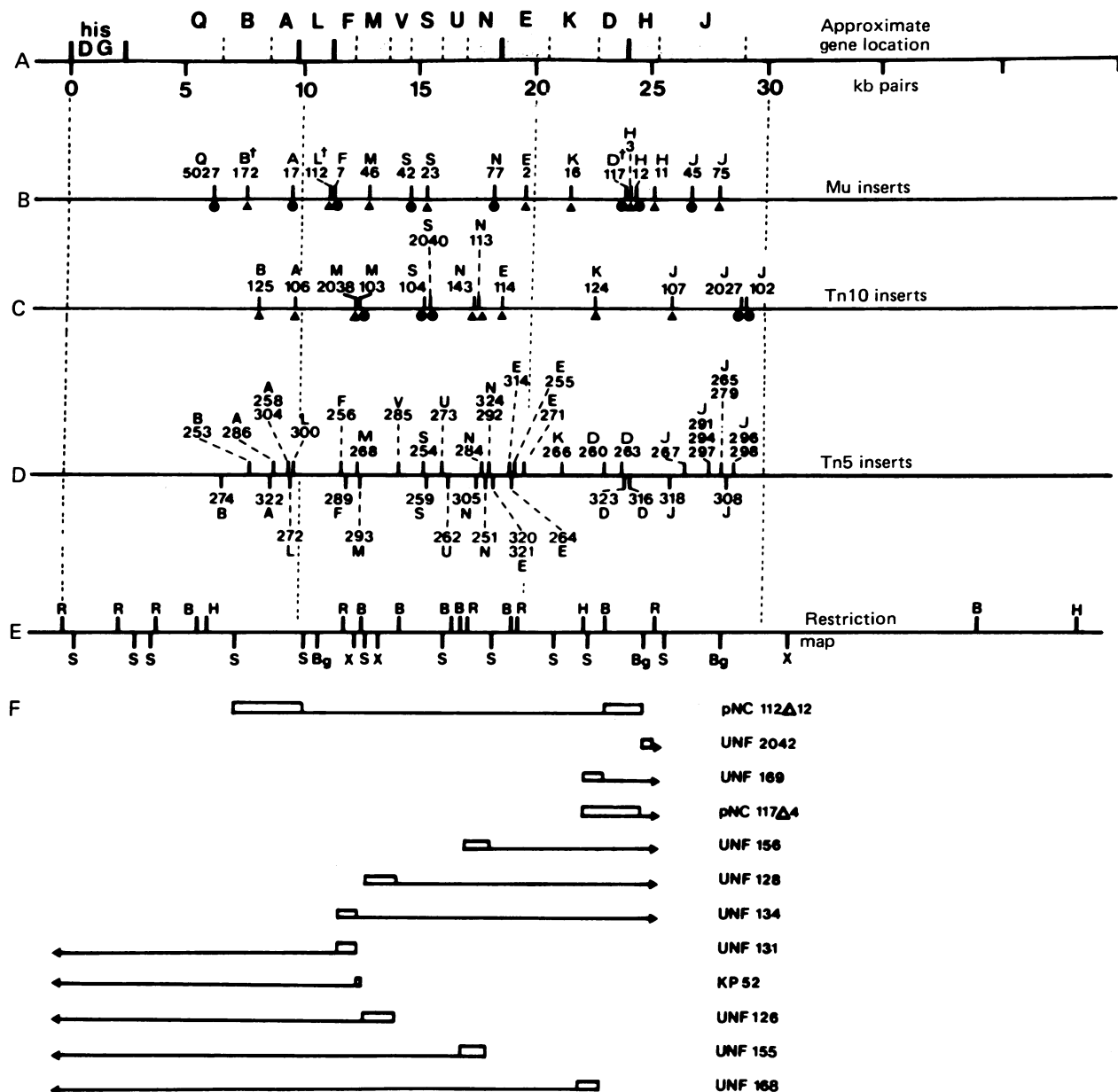


FIG. 4. Physical map of *nif* mutations in the *K. pneumoniae* chromosome. (A) Map of the physical locations of *nif* genes. The minimal size of each *nif* gene (except *nifQ* and *nifV*) was estimated from the distance between insertions in the same gene; the locations of gene boundaries was estimated from distances between insertions in adjacent genes. Solid vertical lines represent boundaries to which we can assign an accuracy of  $\pm 150$  base pairs. Broken vertical lines represent approximate gene boundaries, drawn halfway between the two closest insertions in two adjacent *nif* genes.

(B) Map of the locations of Mu insertions into *nif* genes. Above each location is the number of the pRD1 derivative containing the Mu insertion and the gene to which the mutation has been assigned by complementation analysis. Numbers marked with <sup>†</sup> are from the pNC series of derivatives of pCE1 (3); unmarked numbers are from the pLS series of derivatives of pCE1 (3). *nifQ*5027 (1) is the allele number of a *Muc*<sup>ts</sup> insertion in the *K. pneumoniae* chromosome. Below the location of each insertion, ● indicates that the Mu insertion is oriented as presented in Fig. 1. ▲ indicates the reverse orientation.

(C) Map of the locations of Tn10 insertions into *nif* genes. Above each location is the number of the pMF1 derivative containing the Tn10 insertion and the gene to which the mutation has been assigned by complementation analysis (2). Numbers 143, 2027, 2038, and 2040 are the strain numbers of the UNF series of *K. pneumoniae nif* mutants which contain a Tn10 insertion (2). Below each location, ▲ indicates that the Tn10 insertion is oriented as presented in Fig. 1. ● indicates the reverse orientation.

(D) Map of the locations of Tn5 insertions into *nif* genes. Above each location is the number of the pMF1 derivative containing the Tn5 insertion and the gene to which this mutation has been assigned by complementation analysis (2). Because the restriction enzymes we used to map the locations of the Tn5 insertions cleaved Tn5 symmetrically, this analysis did not determine the orientation of Tn5 insertions.

(E) Restriction map of the *his-nif* region of the *K. pneumoniae* chromosome. Details of the construction of this map will be presented elsewhere. R, *EcoRI*; H, *HindIII*; S, *Sal I*; X, *Xho I*; Bg, *Bgl II*; B, *BamHI*.

(F) Map of the end-point regions of *nif* deletions. The boxes indicate the region to which the end point of the deletion has been assigned. Numbers refer to the strains and plasmids containing the *nif* deletion (2, 3). Arrows indicate the direction in which the deletion extends. UNF2042 is a *nif* inversion mutant of *K. pneumoniae* (ref. 2; R. Dixon and M. Merrick, personal communication).

two particular restriction sites for the end point of each *nif* deletion (data not shown).

### DISCUSSION

Using the procedures described above, we have determined the location of 86 *nif* mutations caused by the insertion of the transposable elements Tn5 and Tn10 and the bacteriophage Mu. We have also mapped the end points of 13 *nif* deletions and 1 *nif* inversion. The results of our mapping studies are compiled in Fig. 4 which shows (i) the approximate location of each *nif* gene, (ii) the sites of insertion of transposable elements in relation to the mapped restriction sites, (iii) the restriction map of the *his-nif* region of the *K. pneumoniae* chromosome for selected restriction endonucleases, and (iv) the end-point region of *nif* deletions and one *nif* inversion in relation to the mapped restriction sites. The *nif* gene order shown in Fig. 4 is the same as the order established by several laboratories using classical deletion mapping procedures (1–3). The minimal size of the entire *nif* gene cluster is 23 kb. The maximal separation between insertions in two adjacent genes (*nifM* and *nifV*) is 1.5 kb, eliminating the possibility of large discontinuities in the *nif* gene cluster. Accurate locations for the boundaries between *nifL* and *nifF*, *nifN* and *nifE*, and *nifD* and *nifH* could be determined because, in these cases, insertions in the two adjacent genes mapped closely to each other. A minimal size for each gene (except *nifQ* and *nifV*) could be assigned because we mapped more than one insertion in each gene. Maximal sizes for each *nif* gene (except *nifQ* and *nifJ*) could be assigned because we had mapped insertions in each gene. Our gene size estimates are in accord with the size estimates of the polypeptide products of *nif* genes J, H, D, K, E, N, S, and F determined by Roberts *et al.* (29) on the basis of polyacrylamide gel electrophoresis. Our data do not rule out the possibility that additional small *nif* genes (0.3–0.5 kb) exist within the *nif* gene cluster and have not yet been identified.

The validity of the “physical” mapping procedure presented here depends upon two testable assumptions: (i) that the sizes and the order of the restriction fragments in the *nif* plasmids are the same as the sizes and the order of the restriction fragments in the *his-nif* region of the *K. pneumoniae* chromosome, and (ii) that the structures of the transposable elements are conserved both during transposition and during DNA replication following transposition. We have shown the sizes and the order of the *Bam*HI, *Sal*I, *Hind*III, *Xho*I, *Bgl*II, and *Eco*RI fragments are identical in the *K. pneumoniae* chromosome, in the conjugative plasmids pRD1 and pMF1, and in the hybrid plasmids pCRA37, pCM1, and pSA30 (unpublished data). We have also shown that the restriction maps of Tn5, Tn10, and Mu following transposition to pRD1 and to pMF1 are identical to the published restriction maps of these three transposable elements.

Physical mapping of the insertion sites of transposable elements provides several distinct advantages over classical mapping procedures. (i) Physical mapping yields more information than deletion mapping because in deletion mapping the actual distance (in base pairs) separating deletion end points are not known. (ii) Physical mapping is especially useful for mapping mutations conferring phenotypes that are difficult to monitor. For example, the nodulation “+” phenotype of *Rhizobium meliloti* can only be observed by inoculating individual alfalfa plants with bacterial strains and incubating the plants for 4–6 weeks to detect the presence or absence of nodule formation. In order to construct a fine structure map of nodulation genes in *R. meliloti* by classical genetic techniques, it would be necessary to test hundreds of individual exconjugants from many crosses by using the nodule formation assay. In contrast, the use of Tn5 to make fine-structure maps of nodu-

lation genes in *R. meliloti* (H. Meade, personal communication) eliminates the necessity of using the nodulation assay. (iii) This physical mapping method is the only definitive method that can be used in bacterial species in which techniques for conducting deletion mapping have not been devised.

One utility of the correlated genetic and physical *nif* maps is that identified restriction fragments can be used as physical probes for each *nif* gene. These fragments can be used in hybridization experiments with *in vivo nif* mRNA to monitor the kinetics of *nif* transcription.

We thank W. Brill, R. Dixon, C. Elmerich, M. Filser, and M. Merrick for providing *nif* mutant strains, plasmids, or results prior to publication, S. Aull for constructing FMA185, P. Bingham for advice concerning labeling DNA *in vitro* and hybridization techniques, N. Kleckner for  $\lambda$ :Tn10 DNA, N. Schaff for an *E. coli*::Muc<sup>ts</sup> lysogen, and J. Salstrom for constructive criticism of the manuscript. This work was supported, in part, by a North Atlantic Treaty Organization grant to F.C.C. and F.M.A. and by National Science Foundation Grant PCM78-15450 to F.M.A.

1. MacNeil, T., MacNeil, D., Roberts, G. P., Supiano, M. A. & Brill, W. J. (1978) *J. Bacteriol.* **136**, 253–266.
2. Merrick, M., Filser, M., Kennedy, C. & Dixon, R. (1978) *Mol. Gen. Genet.* **165**, 103–111.
3. Elmerich, C., Houmard, J., Sibold, L., Manheimer, I. & Charpin, N. (1978) *Mol. Gen. Genet.* **165**, 181–189.
4. Dixon, R., Kennedy, C., Kondorosi, A., Krishnapillai, V. & Merrick, M. (1977) *Mol. Gen. Genet.* **157**, 189–198.
5. Kennedy, C. (1977) *Mol. Gen. Genet.* **157**, 199–204.
6. St. John, R. T., Johnston, N. M., Seidman, C., Garfinkel, D., Gordon, J. K., Shah, V. K. & Brill, W. J. (1975) *J. Bacteriol.* **121**, 759–765.
7. Streicher, S., Gurney, E., & Valentine, R. C. (1971) *Proc. Natl. Acad. Sci. USA* **68**, 1174–1177.
8. Cannon, F. C., Redel, G. E. & Ausubel, F. M. (1977) *Proc. Natl. Acad. Sci. USA* **74**, 2963–2967.
9. Cannon, F. C., Riedel, G. E. & Ausubel, F. M. (1979) *Mol. Gen. Genet.*, in press.
10. Barth, P. T. & Grinter, N. J. (1977) *J. Mol. Biol.* **113**, 455–474.
11. Dougan, G. & Sherratt, D. (1977) *Mol. Gen. Genet.* **15**, 151–160.
12. Inselburg, J. (1977) *J. Bacteriol.* **129**, 482–491.
13. Bachman, B. J. (1972) *Bacteriol. Rev.* **36**, 525–557.
14. Cannon, F. C., Dixon, R. A. & Postgate, J. R. (1976) *J. Gen. Microbiol.* **93**, 111–125.
15. Streicher, S., Gurney, E. & Valentine, R. C. (1972) *Nature (London)* **239**, 495–499.
16. Dixon, R. A., Cannon, F. C. & Kondorosi, A. (1976) *Nature (London)* **260**, 268–271.
17. Allet, B., Blattner, F., Howe, M., Magazin, M., Moore, D., O'Day, K., Schultz, D. & Schumm, J. (1977) in *DNA Insertion Elements, Plasmids, and Episomes*, eds. Bukhari, A. I., Shapiro, J. A. & Adhya, S. L. (Cold Spring Harbor Laboratory, Cold Spring Harbor, NY), pp. 745–748.
18. Jorgensen, R. (1978) Dissertation (Univ. of Wisconsin, Madison, WI).
19. Jorgensen, R. A., Berg, D. E., Allet, B. & Reznikoff, W. S. (1979) *J. Bacteriol.* **137**, 681–685.
20. Marmur, J. (1961) *J. Mol. Biol.* **3**, 208–218.
21. Greene, P. J., Betlach, M. C., Goodman, H. M. & Boyer, H. W. (1974) in *Methods in Molecular Biology*, ed. Wickner, R. B. (Dekker, New York), Vol. 7, pp. 87–111.
22. Southern, E. M. (1975) *J. Mol. Biol.* **98**, 503–517.
23. Tanaka, T. & Weisblum, B. (1975) *J. Bacteriol.* **121**, 354–362.
24. Rigby, P. W. J., Dieckmann, M., Rhodes, C. & Berg, P. (1977) *J. Mol. Biol.* **113**, 237–251.
25. Maniatis, T., Jeffrey, A. & Kleid, D. (1975) *Proc. Natl. Acad. Sci. USA* **72**, 1184–1188.
26. Gillespie, D. & Spiegelman, S. (1965) *J. Mol. Biol.* **12**, 829–842.
27. Denhardt, D. (1966) *Biochem. Biophys. Res. Commun.* **23**, 641–646.
28. Botchan, M., Topp, W. & Sambrook, J. (1976) *Cell* **9**, 269–287.
29. Roberts, G. P., MacNeil, T., MacNeil, D. & Brill, W. J. (1978) *J. Bacteriol.* **136**, 267–279.